BIOCHEMISTRY
including biophysical chemistry & molecular biology

Article

pubs.acs.org/biochemistry

Water Channel in the Binding Site of a High Affinity Anti-Methotrexate Antibody

Susan Gayda,[†,⊥] Kenton L. Longenecker,[‡,§,⊥] Sharmila Manoj,[†] Russell A. Judge,[‡,§] Sylvia C. Saldana,[†] Qiaoqiao Ruan,[†] Kerry M. Swift,[†] and Sergey Y. Tetin*[,†]

[†]Diagnostics Research, Abbott Diagnostics Division and [‡]Structural Biology, Global Pharmaceutical Research and Development, Abbott Laboratories, Abbott Park, Illinois 60064, United States

ABSTRACT: In the present study, we report the structure of the free and drug-bound Fab fragment of a high affinity anti-methotrexate antibody and perform a thermodynamic analysis of the binding process. The anti-methotrexate Fab fragment features a remarkably rigid tunnel-like binding site that extends into a water channel serving as a specialized route to move solvent out and into the site upon ligand binding and dissociation. This new finding in antibody structure−function relationships directly relates to the fast association (1×10^7 M^{-1} s^{-1}) and slow dissociation (4×10^{-5} s^{-1}) rates determined for mAb ADD056, resulting in a very strong binding with a $K_D \sim 3.6$ pM at 20 °C. As follows from the X-ray data analysis, the methotrexate-antibody complex is stabilized by an extended network of hydrogen bonds and stacking interactions. The analysis also shows structural involvement of the CDR H3 in formation of the water channel revealing another important role of this hypervariable region. This suggests a new direction in natural affinity maturation and opens a new possibility in antibody engineering. Methotrexate is a widely used therapeutic agent for many malignant diseases and inflammatory disorders. Unfortunately, it may also interfere with central aspects of metabolism and thereby cause inevitable side effects. Therefore, methotrexate therapy requires careful monitoring of drug blood levels, which is traditionally done by immunoassays. An understanding of the structure−function properties of antibodies selected for drug monitoring substantiates the performance and robustness of such tests.

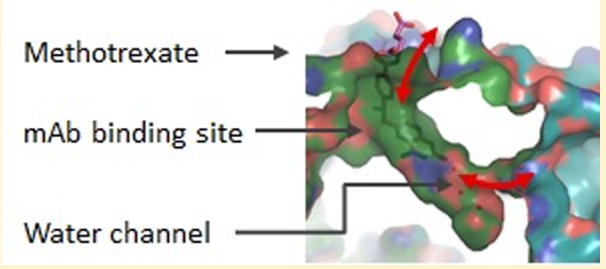

The vast diversity of genes that encode antibody variable regions provides for a large variety of antibody binding site architectures.[1] Scores of various target molecules bind to subsequent highly specific antibodies with subnanomolar affinities. Binding of small organic molecules presents a special case of precise structural recognition.[2] In the immunological literature, such ligands are identified as *haptens* because they cannot induce an immune response without being attached to a much larger protein carrier.[3] Haptens have a limited number of charged or polar groups and a diminutive surface. Thus, antibodies accommodate them in deep pocket-type binding sites with specific geometry that perfectly fits the shape of the ligand. Such binding processes often require conformational malleability of the antibody binding site.[2,4−7] In the case of lock-and-key binding, penetration of a ligand into the rigid binding site would require effective displacement of water molecule(s) that fill the site in the absence of ligand. For instance, the opening to the rigid binding site of anti-digoxin antibody 26-10 is wide enough to allow for the solvent to exchange.[8] We found a very different situation when we studied the structure and thermodynamic properties of a high affinity mouse monoclonal antibody that is used for clinical monitoring of methotrexate, a well-known drug with a strong cytostatic effect.[9−11]

Here, we present the crystal structure and thermodynamic characterization of this anti-methothexate, mAb ADD056. It strongly binds the drug, featuring a dissociation constant (K_D) in the low picomolar range. The tight binding results from a complex hydrogen bonding network within the binding site, which exclusively involves the 2,4-diaminopteridine (DA-pteridine) ring of methotrexate (Figure 1). Further stacking

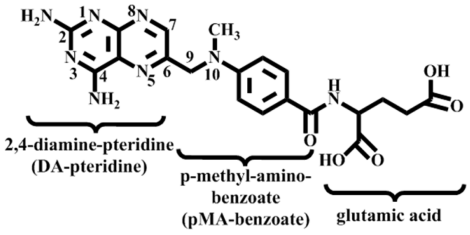

Figure 1. Sketch of the chemical structure of methotrexate, describing the terminology used throughout the manuscript.

interactions stabilize the *p*-methylaminobenzoate (pMA-benzoate) moiety, whereas methotrexate's glutamic acid tail extends free to the exterior of the binding site. Altogether, the complex is stabilized by $\Delta G = (-63.7 \pm 3.5)$ kJ mol^{-1}.

Mechanistically, the fast association rate ($k_{on} \sim 1 \times 10^7$ M^{-1} s^{-1} at 20 °C) substantiates the efficiency of the complex

Received: January 31, 2014
Revised: May 7, 2014
Published: May 15, 2014

   dx.doi.org/10.1021/bi5001382 | *Biochemistry* 2014, 53, 3719−3726

formation. The association reaction is apparently facilitated by a water channel that connects the interior of the binding site with the Fab's surface enabling easy escape of the water molecules from the site upon methotrexate binding. Reciprocally, dissociation of the ligand requires moving the water through the channel back into the binding site.

The water channel is established in part by the heavy chain complementarity determining region (CDR) H3. This fact allows us to speculate that formation of the water channel has directly resulted from affinity maturation of the given antibody.[1,12]

MATERIALS AND METHODS

A series of anti-methotrexate hybridomas were made in house by J.D. Tyner and R.N. Ziemann at Abbott Diagnostics Division in the early 1990s. Hybridoma producing mAb ADD056 was selected based on the antibody affinity to methotrexate and its secretion level.

Sequencing Anti-Methotrexate mAb ADD056. Messenger RNA (mRNA) from hybridoma ADD056 was purified by Oligotex (Qiagen, Germantown, MD) using a protocol as recommended by the manufacturer. Purified mRNA was reverse transcribed into cDNA, which was then amplified with a set of mouse IgG specific primers (Novogen, now sold by EMD Millipore, Billerica, MA). Positive PCR products were gel purified and cloned into pCR TOPO 2.1 TA vector (Life Technologies, Grand Island, NY). The plasmid DNA was purified from transformed bacterial cells and the sequence of the V_H or V_L inserts were identified by sequencing using M13 reverse primer and Big Dye Terminator sequencing kit (Applied Biosystems, Foster City, CA).

Cloning Heavy and Light Chain Genes into Transient Expression Plasmid. Linear DNA encoding variable domains of heavy and light chain (V_L and V_H) of mAb ADD056 were amplified by PCR using Deep Vent Polymerase (NEB, Ipswitch, MA) to generate blunt ends. The V_L PCR product was gel-purified and digested with Nru I restriction enzyme and ligated in frame with the upstream mouse kappa signal and downstream mouse constant kappa region encoded by the expression vector, pBOS-Vk, which was digested with NruI-AfeI. Similarly, the NruI digested mouse V_H PCR product was ligated in frame with the upstream mouse heavy chain signal sequence and downstream constant region of mouse IgG2a on the pBOS-m2a expression vectors digested with NruI-AfeI. The presence of the desired inserts on both plasmids was confirmed by sequencing as described above using appropriate primers on either sides of the region of interest.

Transient Transfection for Anti-Methotrexate Antibody. Plasmids were purified using Gigaprep kits (Qiagen, Valencia, CA) according to the manufacturer's instructions. PEI-mediated (Polysciences, Warrington, PA) transfections were performed adding the purified plasmids to HEK293 cells cultured in 293 Freestyle Medium (Life Technologies, Grand Island, NY). HEK cells were passaged the day before transfection to achieve a cell density of 10^6 cells/ml on the day of transfection. DNA:PEI were mixed in ratios of 1:2 and allowed to incubate at room temperature for 10 min prior to addition to cells. The final concentration of the DNA was 1 μg/mL. Transfections were allowed to proceed for 7−10 days before the supernatants were harvested.

Purification of Anti-Methotrexate Antibody. The harvested supernatants were clarified by centrifuging at 8000 rpm for 20 min and filtered through a 0.45 μm filter (Corning, Corning, NY). Supernatants were diluted with PBS (Sigma, St Louis, MO) prior to loading onto a Protein A column (Pierce, Rockford, IL). After washing the column, bound antibodies were eluted with 0.1 M citric acid pH 2.8 and immediately neutralized. Eluted fractions were analyzed by SDS-PAGE gel and selected fractions were pooled and dialyzed at room temperature three times in PBS, pH 7.2. The final purified antibody was filtered and stored in a −80 °C freezer.

Generation of Fab Fragments. Anti-methotrexate antibody was digested in a 100:1 IgG:papain mixture using agarose-immobilized papain (Pierce, Rockford, IL). The papain resin was washed two times in digestion buffer (PBS, 1 mM DTT, 1 mM EDTA) before adding the IgG stock solution. The digestion mixture was incubated at 37 °C under slow stirring, and the reaction progress was monitored by HPLC (Beckmann Gold 126 HPLC system) using a G2000 SWxI column (Tosoh Corporation). Proteolysis was stopped after 6 h by separating the papain resin from the solution. Residual IgG and Fc fragments were removed by Protein A affinity chromatography. Purified Fab was dialyzed into Tris−HCl buffer (20 mM Tris, pH 7.3, 50 mM NaCl). The final purity of the mAb ADD056 and its Fab fragment was higher than 95% as determined by SDS PAGE and HPLC. To prepare methotrexate:Fab complex for crystallization, free Fab was mixed with 20% molar excess of methotrexate and concentrated to 20 mg/mL using Amicon Ultra centrifugal filters (Millipore, Billerica. MA).

X-ray Crystallography. Crystals of the methotrexate:Fab complex and the Fab alone were grown using the sitting drop vapor diffusion method at 23 °C. In both instances, a 20 mg/mL protein solution was mixed in a 1:1 (v/v) ratio with reservoir solutions to form the sitting drop. The drop was then equilibrated against the solution in the reservoir. Free Fab and methotrexate:Fab complex were crystallized in 0.1 M citric acid, pH 3.5, reservoir solution using 2 M ammonium sulfate and 3 M sodium chloride, respectively. Crystals were observed after three weeks in both cases. For cryoprotection, crystals were transferred into their respective reservoir solutions containing 20% (v/v) propylene glycol and vitrified in liquid nitrogen. The X-ray diffraction data sets were collected at the 17-ID IMCA CAT beamline at the Advanced Photon Source (Argonne National Laboratory, Argonne, IL) under gaseous nitrogen at 100 K.

Diffracted intensities were processed using autoPROC,[13] and the structure was solved by molecular replacement with related V_HV_L and C_HC_L coordinates using MOLREP[14] in the CCP4 program suite.[15] The model was rebuilt using COOT[16] with ligand fitting by AFITT,[17] and refined against structure factors using the programs REFMAC5[18] and autoBUSTER.[19] Figures were prepared using the program PYMOL (DeLano Scientific, Schroedinger Inc.).

Equilibrium Binding Characterization. A methotrexate-fluorescein conjugate was prepared as previously described.[20] Experiments were performed using a SLM8100 photon counting spectrofluorimeter equipped with prism polarizers. The conjugate was excited at 480 nm (4 nm bandwidth slits) and the emission was monitored through a 530/25 nm bandwidth filter. Binding of anti-methotrexate antibody was monitored by following the methotrexate-fluorescein anisotropy, which increases 10-fold from 0.02 to 0.2 upon binding to the antibody. A 25% binding induced quenching was taken into account when processing anisotropy data. All experiments were carried out in HBS-EP buffer (0.01 M HEPES, pH 7.4, 0.15 M NaCl, 3 mM EDTA, 0.005% Surfactant P20; GE Healthcare,

Little Chalfont, U. K.), if not indicated otherwise. In the equilibrium binding experiments, an incrementally increasing concentration of antibody was titrated into the methotrexate-fluorescein solution, which was kept at a constant concentration of 50 pM. Details of the procedures and data evaluation are described elsewhere.[21]

Briefly, room temperature equilibrium experiments were carried out by monitoring the anisotropy change of methotrexate-fluorescein upon increasing Fab ADD056 concentration. The fraction bound (F_b), relates directly to the measured anisotropy as described by

$$F_b = \frac{r - r_{free}}{(r_{bound} - r)q + r - r_{free}} \quad (1)$$

where r is anisotropy at any given concentration of the binding sites; r_{free} and r_{bound} are anisotropy values for free and bound methotrexate-fluorescein; and q is the quenching factor.

The target concentrations of methotrexate-fluorescein in our equilibrium binding experiments were equal or slightly below the value of the expected dissociation constant. In these cases, the binding data were fit to the simple binding model $F_b = S/(K_D+S)$ as previously described.[21]

If such concentration levels were not achievable due to the detection limit imposed by the fluorescence efficiency of methotrexate-fluorescein, the equilibrium dissociation constant K_D at room temperature was estimated from stoichiometric binding data using the quadratic equation:[21]

$$F_b = \frac{K_D + S_t + L_t - \sqrt{(K_D^2 + 2K_DS_t + 2K_DL_t + S_t^2 - 2S_tL_t + L_t^2)}}{2S_t} \quad (2)$$

K_D values at other temperatures were calculated from the kinetic rates.

Kinetic Studies. The complex association, on-rates (k_{on}) were measured by following the decrease in fluorescence intensity of methotrexate-fluorescein at magic angle (0/55°), using a BioLogic stopped-flow module SFM-3 (Claix, France) mounted on a SLM-Aminco AB-2 fluorimeter. A 100 nM solution of methotrexate-fluorescein and 115 nM solution of Fab ADD056 in PBS were mixed in equal volumes. The on-rate was determined for temperatures between 12 and 45 °C. Complex dissociation, off-rates (k_{off}) were determined by the following procedure. A mixture of 100 nM methotrexate-fluorescein and 200 nM Fab was prepared and allowed to equilibrate. The equilibrium was disturbed by diluting the mixture 50-fold into 200 nM unlabeled methotrexate solution to prevent reassociation. The dissociation of the complex was monitored by the decrease in fluorescein anisotropy recorded with the SLM 8100 spectrofluorometer. The reaction was measured at different temperatures between 15 and 40 °C.

$$\frac{d[LS]}{dt} = -(+)[LS]_0 e^{-t/\tau} \text{on(off)} \quad (3)$$

Time traces for on (off) reaction were fitted to a single exponential function. With τ being the reaction lifetime and $[LS]$ the concentration of ligand:binding site complex. The subscript 0 indicates initial concentrations.

Association of methotrexate tracer to anti-methotrexate Fab is described by a bimolecular reaction:

$$\frac{d[LS]}{dt} = k_{on}[L][S] \quad (4)$$

with the solution:

$$k_{on} = \frac{1}{\tau(\ln 2)(S_t - L_t)} \ln\left[\frac{2(S_t - L_t/2)}{S_t}\right]$$

Here, S, L, S_t and L_t indicate free and total concentrations of binding sites and ligand, respectively.

Dissociation of the complex follows simple first order kinetics with the solution $k_{off} = 1/\tau_{off}$.

RESULTS

Overall X-ray Structure of the Fab and Assignment of Its CDR. To elucidate the molecular basis of the Fab ADD056:methotrexate complex formation, the Fab fragment was crystallized in its apo- and ligand-bound form. The data collection and refinement strategies are compiled in Table 1.

Table 1. X-ray Data and Refinement

	free Fab	methotrexate:Fab complex
X-ray diffraction data		
space group	$P2_13$	$P2_13$
unit cell length (Å)	144	143
resolution	2.8	2.4
observations	178 657	384 393
unique	25 192	
completeness (%)	99.4	100
mean diffraction signal (I/σ)	10	23
R_{merge} (%)	14.9	6.6
model refinement		
reflections (work/free)	23763/1275	36985/1952
R_{factor} (work/free %)	18.4/20.9	18.7/21.8
protein residues	433	433
mean B value	42	52
RMSD ideal bond length (Å)	0.01	0.01
RMSD ideal bond angles (degrees)	1.32	1.36

The X-ray structures of apo-form and the complex were determined at a resolution of 2.8 and 2.4 Å, respectively. Both crystals belong to the cubic space group $P2_13$, featuring a similar unit cell length of 144.4 and 143.4 Å. The asymmetric units contain both variable (V_H and V_L) and constant (C_H and C_L) domains of Fab heavy and light chains in their typical fold. The anti-methotrexate Fab consists of 433 amino acid residues, which are visible in the electron density maps for both apo and complex structures. The electron density map of the complex features additional electron density between the variable domains, which fits readily to a single methotrexate molecule (Figure 2a).

The three-dimensional structures of all CDRs, except H3, are similar to previously identified canonical structures. Their length and sequence was determined using the AbM definition (Antibody structure modeling software, Oxford Molecular Group, Inc.). The CDR loops L1, L3, H1, and H2 belong to Chothia's classes 4, 1, 2, and 3A.[22,23] A more recent clustering of CDR conformations introduced by North et al., classifies CDR structures based on their length and conformation.[24] The authors identified several new canonical structures, among them a cluster that includes the conformation of the L2 loop found in the anti-methotrexate Fab fragment ADD056. According to this classification hypervariable regions L1, L2, L3, H1, and H2 belong to clusters L1-16-1, L2-8-5, L3-9-*cis*7-1,

dx.doi.org/10.1021/bi5001382 | *Biochemistry* 2014, 53, 3719−3726

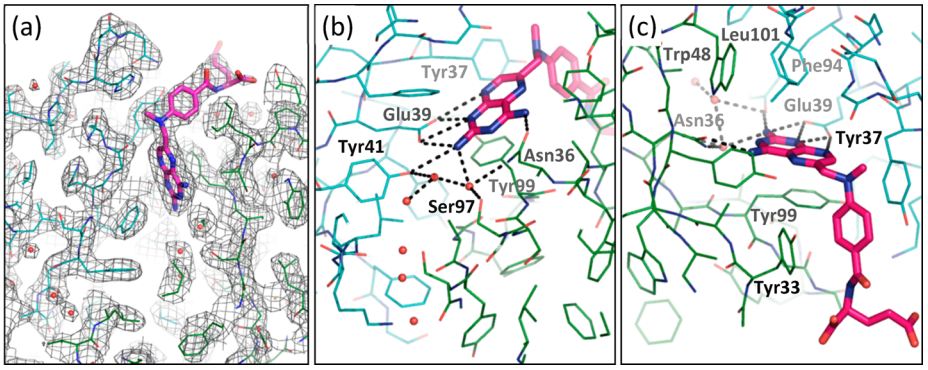

Figure 2. Interactions between methotrexate and Fab mAb ADD056 in the binding site. Heavy (green) and light (cyan) chain are depicted as lines; the ligand (magenta) is represented by sticks. (a) Electron density for the binding pocket, depicted at a 2mFo-DFc contour level of 1σ. (b) Hydrogen bond network around the methotrexate DA-pteridin moiety. (c) Steric fit of methotrexate's pMA-benzoate group. Note: Recorded absorption spectra of antibody-bound methotrexate confirmed that the ligand's pteridin moiety is neutral in both crystallization buffer (pH 3.5) and HBS-EP buffer (pH 7.4). The hydrogen bonds to methotrexate's N1 and N8 are established if $Glu39_L$ donates the hydrogen. We assume that the micro environment of $Glu39_L$ increases its pK_a above 7.4.

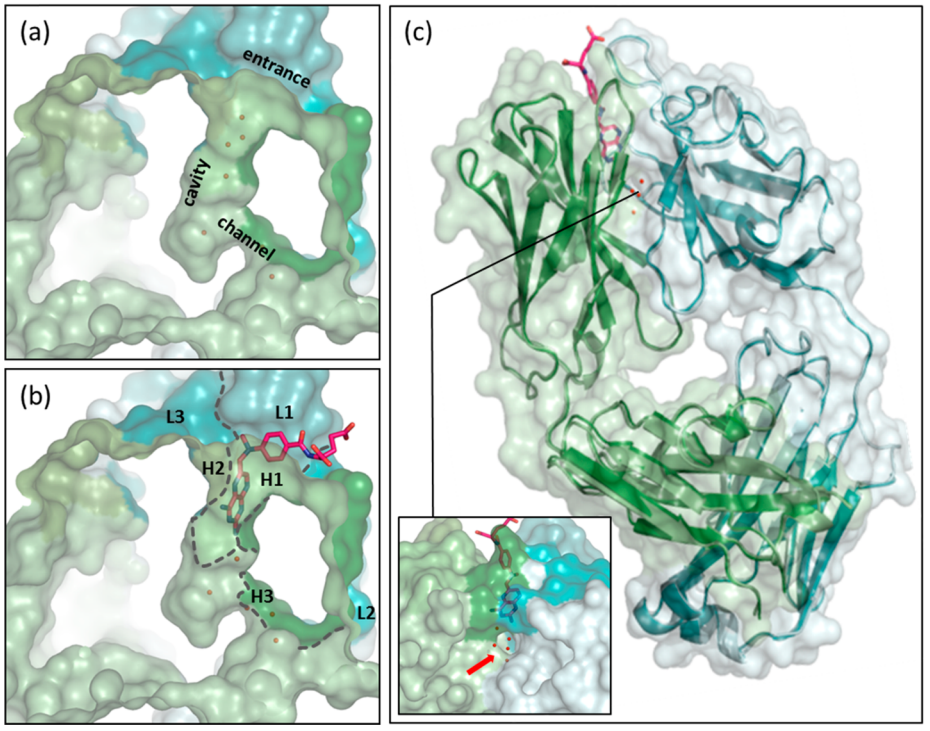

Figure 3. X-ray structures of Fab ADD056 heavy (green) and light (cyan) chains. (a) Surface model of the binding domain without and (b) with ligand bound. Entrance, cavity, and water channel are marked. Different shadings and dotted lines indicate CDR loops H1−H3 (green) and L1−L3 (cyan). (c) Overlay of cartoon and surface models for the X-ray structures of free (light) and bound state (dark). Inset shows the secondary entry portal of the water channel, which is marked by a red arrow. Red spheres represent solvent molecules.

H1-14-1, and H2-10-2. The hypervariable loop H3 has a length of 7 amino acids. Its anchor region is atypical and cannot be classified by this method.[24]

Description of the Binding Site. Structurally, the binding site is shaped like a deep tunnel containing an elongated narrow entrance, a close-fitting cavity, and a water channel (Figure 3a). The entrance extends about 16 Å along the horizontal interface of V_L and V_H with the walls built by all CDRs but L2. The opening leads into a tight cavity which reaches approximately 22 Å deep into the protein matrix. About a third above the cavity's bottom, it branches into a channel, which emerges as a secondary entry portal on the Fab's surface just below the interface of the L2 and H3. The channel is formed by sections of β-sheets of the V_L and V_H framework, but in large part also by H3, which emphasizes the structural importance of this hypervariable region (Figure 3b). The residues outlining the inner channel contribute both backbone and side chains to the channel surface. $Ser97_H$ and $Tyr41_L$ are located in the bend between binding cavity and the pocket, forming the "entrance" into the channel. The middle section of the channel is lined by the side chains of $Leu51_L$, $Ala104_H$, and $Ser106_H$. Their backbone moieties, together with the backbone from $Try105_H$, form the polar "exit" region. Its opening is located at the center of the vertical interface of the variable domains (Figure 3c), and the channel entrance-to-exit axis is almost perpendicular to the longitudinal axis of the binding cavity. The resolution of the

dx.doi.org/10.1021/bi5001382 | *Biochemistry* 2014, 53, 3719−3726

apo-structure limits the exact assignment of the solvent molecules present in the channel in the ligand-free Fab fragment. However, the low level of electron density for a few of these molecules suggests some ambiguity in their position, although they are involved in diverse interactions with the protein matrix of both chains.

The V_HV_L domains for the Apo and methotrexate-bound structures align closely with an RMSD of 0.31 Å for main chain atoms, suggesting a highly rigid binding site that is structurally not affected by methotrexate binding (Figure 3c). The ligand displaces solvent from the binding cavity and a few amino acid side chains shift slightly to accommodate this change. Amino acid side chains of $Glu39_L$, $Tyr41_L$, $Asn36_H$, and $Ser97_H$ form an intricate network of hydrogen bonds with the methotrexate DA-pteridine ring, tightly fixating the ligand in the cavity (Figures 1 and 2b). Most moieties of the methotrexate molecule have several potential interaction partners. The DA-pteridine 2-position amino group forms a hydrogen bond with $Glu39_L$, which in its turn, interacts with N^1 and N^8 atoms of the DA-pteridine. The shape of the absorption spectrum of antibody-bound methotrexate at crystallization conditions confirms that its pteridin moiety remains neutral. Therefore, we assume that the pK_a of $Glu39_L$ is increased above 7.4 and it donates hydrogen to these interactions. A second hydrogen bond connects the 2-position amino group with $Tyr41_L$. In addition, $Tyr41_L$ makes hydrogen bonds with two water molecules integrated in the complex. One of these waters interacts with $Ser97_H$ and $Asn36_H$. Besides that, the $Asn36_H$ side chain forms a sole hydrogen bond with the 4-position amino group of the DA-pteridine. Stacking interactions and steric restrictions, provided by $Leu101_L$ and $Phe94_L$ above the DA-pteridine and $Tyr99_H$ below it, further stabilize the complex.

Beyond interactions between protein matrix and DA-pteridine portion, the pMA-benzoic acid moiety is closely embedded between $Tyr33_H$ and $Tyr37_L$, which are conserved residues in the canonical structures of H1 and L1.[24] Methotrexate's glutamic acid moiety is the only part of the ligand that does not form any evident interactions with the protein matrix and extends out of the binding site (Figure 2c). This observation is not surprising because the methotrexate immunogen was prepared by ligating the glutamic acid moiety to the protein carrier.

Thermodynamics in Equilibrium. Solution-phase binding measurements performed at equilibrium revealed a dissociation constant K_D ~3.6 pM (Figure 4a), which reflects the formation of a very tight methotrexate:Fab complex, stabilized by $\Delta G = -RT \ln(1/K_D) \approx -64$ kJ mol^{-1} at room temperature (293 K).

The contribution of entropy and enthalpy to the overall stabilization of the complex was analyzed using Van't Hoff's plot, which requires measuring K_D at different temperatures. For maximum accuracy, equilibrium titration experiments require to keep ligand concentrations close to or lower than the value of the expected K_D.[25] Due to the high binding affinity of the anti-methotrexate antibody, such binding conditions exceed the limits of detection in our experiments, especially at lower temperatures. Thus, the K_D values were calculated from kinetic data using the association (k_{on}) and dissociation (k_{off}) rate constants determined independently at each temperature: $K_D = k_{off}/k_{on}$. Thermodynamic parameters were calculated directly from Van't Hoff's equation (Figure 4b), derived from $\Delta G = \Delta H - T\Delta S$ and $\Delta G = -RT \ln K_A$

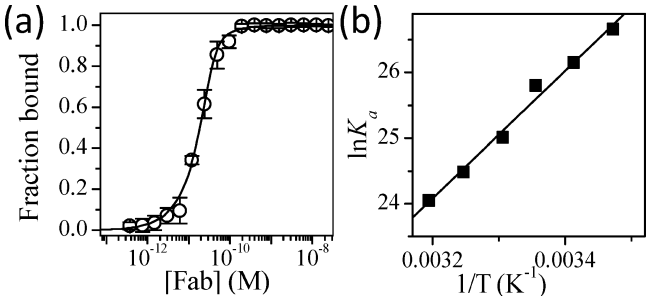

Figure 4. Thermodynamic equilibrium of methotrexate-fluorescein:-Fab of mAb ADD056. (a) Equilibrium titration of Fab into 50 pM methotrexate-fluorescein at ambient temperature. Measured values (symbols) fit to the model described by eq 2 (line) with a dissociation constant K_D of ~3.6 pM. (b) Van't Hoff plot for association constants K_A. Energies were calculated from its linear regression, according to eq 5.

$$\ln K_A = \frac{\Delta S}{R} - \frac{\Delta H}{R}\frac{1}{T} \tag{5}$$

where $K_A = 1/K_D$ is the association constant, R is the universal gas constant, T is the absolute temperature, and ΔS and ΔH are the changes in entropy and enthalpy upon complex formation, respectively.

As follows from these calculations, at room temperature, the complex is stabilized by a large reduction in enthalpy (ΔH = (−81.0 ± 4.4) kJ mol^{-1}). A smaller increase in the entropy term counterweights this effect with $-T\Delta S$ = (17.3 ± 4.3) kJ mol^{-1} at 293 K. Therefore, the reduction in Gibbs free energy upon complex formation is ΔG = (−63.7 ± 3.5) kJ mol^{-1}, which is in good agreement with ΔG calculated directly from the K_D measured at equilibrium at the same temperature (ΔG ~ 64 kJ mol^{-1}).

Thermodynamics of the Activated Complex. According to the transition state theory, the reaction rates of methotrexate:Fab complex association (k_{on}) and dissociation (k_{off}) are limited by energetic activation barriers. The amplitude and nature of these barriers can be revealed by studying the reaction kinetics at various temperatures. The relationship between the rate coefficients and activation energies is described by the Arrhenius equation

$$\ln k = \ln A^* - \frac{\Delta H^*}{R}\frac{1}{T} \tag{6}$$

whereby, A^* is the Arrhenius factor, which relates to the changes in activation entropy ΔS^* as given by the Eyring equation

$$A^* = \frac{k_b T}{h} \cdot e^{\Delta S^*/R} \tag{7}$$

Here, k_b is the Boltzmann constant and h is the Planck constant.

Example time traces and Arrhenius plots for complex association and dissociation are shown in Figure 5. A rise in temperature from 12 to 45 °C moderately accelerates k_{on} from 0.9 × 10^7 to 1.9 × 10^7 M^{-1} s^{-1}, indicating a low activation energy barrier for the association of the complex. Indeed, at room temperature (293 K), the activation enthalpy ΔH_{on}^* = (19.0 ± 0.5) kJ mol^{-1} and activation entropy term $-T\Delta S_{on}^*$ = (13.3 ± 0.1) kJ mol^{-1} are rather small, resulting in a free energy barrier of only ΔG_{on}^* = (32.3 ± 1.1) kJ mol^{-1}. In contrast, the dissociation of the complex is accelerated from k_{off} = 0.2 × 10^{-4}

dx.doi.org/10.1021/bi5001382 | Biochemistry 2014, 53, 3719−3726

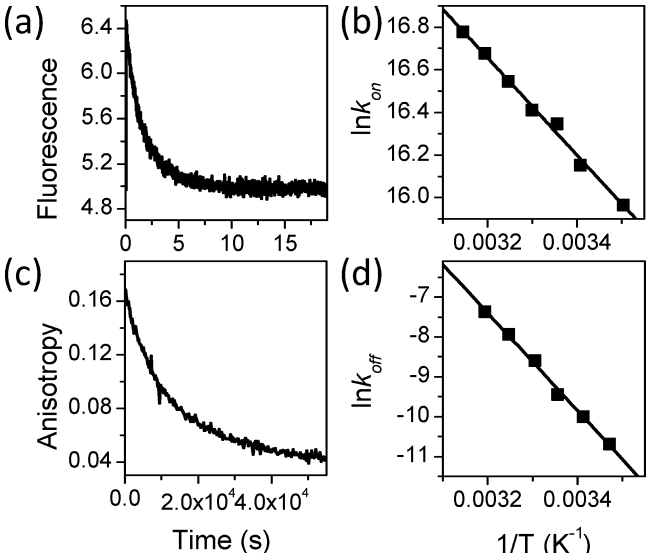

Figure 5. Kinetics of association and dissociation of methotrexate-fluorescein:Fab ADD056 complex. (a) Typical time trace monitoring fluorescence intensity decrease of methotrexate-fluorescein upon complex association at 298 K. (b) Arrhenius plot for on-rates (k_{on}) determined for temperatures between 12 and 45 °C. (c) Typical time trace monitoring anisotropy decrease of methotrexate-fluorescein upon complex dissociation at 298 K. (d) Arrhenius plot for off-rates (k_{off}) determined for temperatures between 15 and 40 °C.

to 6.3×10^{-4} s^{-1} between 15 and 40 °C, a more than 30-fold increase. The high activation energy of $\Delta G_{off}^{*} = (96.1 \pm 5.3)$ kJ mol^{-1} is mainly caused by a barrier in activation enthalpy $\Delta H_{off}^{*} = (101.7 \pm 2.5)$ kJ mol^{-1}. The effect of the increase in the order of the system upon ligand dissociation is rather small with $-T\Delta S_{off}^{*} = (-5.6 \pm 0.2)$ kJ mol^{-1} at 293 K. These results are summarized in Table 2.

Table 2. Thermodynamic Parameters of Methotrexate:Fab ADD056 Complex Formation

	equilibrium[c]	association[c]	dissociation[c]
ΔG^{a} (kJ mol^{-1})	−63.7 ± 3.5	32.3 ± 1.1	96.1 ± 5.3
ΔH^{a} (kJ mol^{-1})	−81.0 ± 4.4	19.0 ± 0.5	101.7 ± 2.5
$-T\Delta S^{a,b}$ (kJ mol^{-1})	17.3 ± 4.3	13.3 ± 0.1	−5.6 ± 0.2

[a]Activation energies. [b]Activation entropy term for 293 K. [c]Errors determined from uncertainty of linear fits in Van't Hoff/Arrhenius plots.

DISCUSSION

Structural Interpretation of the Binding Thermodynamics. The anti-methotrexate mAb ADD056 tightly binds methotrexate with an equilibrium dissociation constant in the low picomolar range ($K_D \sim 3.6$ pM). X-ray analysis of the complex revealed a remarkably rigid binding site featuring a deep binding cavity and a 5 Å wide and 8 Å long water channel that extends perpendicularly to the longitudinal axis of the variable domain and emerges on the surface of the molecule. An intricate network of diverse interactions between methotrexate and protein matrix stabilizes the complex. The actual binding site contains two parts, one of which embeds methotrexate's pMA-benzoate moiety in an elongated narrow entrance and the second of which captures the DA-pteridine portion of methotrexate in a deep cavity. Polar interactions drive the binding process, contributing an enthalpy change of $\Delta H = (-81 \pm 4.4)$ kJ mol^{-1} upon complex formation at room temperature. These stabilizing interactions are considerably opposed by an unfavorable change in the entropy of the system ($-T\Delta S = (17.3 \pm 4.3)$ kJ mol^{-1}), which reduces the overall complex stabilization energy to $\Delta G = -(63.7 \pm 3.5)$ kJ mol^{-1}.

A small enthalpy barrier of the association process ($\Delta H_{on}^{*} = (19.0 \pm 0.5)$ kJ mol^{-1}) explains the fast binding reaction. A small entropy barrier ($-T\Delta S_{on}^{*} = (13.3 \pm 0.1)$ kJ mol^{-1} at 293 K) reflects the increased order of the system upon ligand binding and opposing it, the translocation of solvent molecules from the cavity through the water channel (Figure 3). Minor shifts in the position of certain amino acids side chains may also contribute to the activation entropy.[26]

The elaborate hydrogen bond network and stacking interactions stabilize methotrexate in the binding site causing a very high activation barrier for its dissociation. The high enthalpy barrier of $\Delta H_{off}^{*} = (101.7 \pm 2.5)$ kJ mol^{-1} is only slightly counterweighted by the increase in the system's disorder $-T\Delta S_{off}^{*} = (-5.6 \pm 0.2)$ kJ mol^{-1} at 293 K. Overall, a large activation energy of $\Delta G_{off}^{*} = (96.1 \pm 5.3)$ kJ mol^{-1} is required to break the complex resulting in a slow dissociation rate.

A Secondary Entry Portal As "Solvent Escape Route". In general, the limited number of possible interactions with a small ligand inputs special requirements on the character of the binding protein. Small organic molecules are frequently found in deep pockets or cavities with peculiar shape, which adds strict geometric restraints to the binding force. However, such binding site architectures create additional challenges to the binding process. Penetration of the ligand into the densely packed protein interior requires major conformational adjustments or displacement of the solvent molecules that filled the binding site in the absence of the ligand. Therefore, the induced fit mechanism is very common for antibodies against haptens and small antigens.[2,4−7] In the case of the lock-and-key type of binding, the binding site should have a widely open entrance area allowing solvent to escape, as was observed in anti-digoxin antibody 26-10.[8] The almost perfect overlay of the structures (RMSD Cα V_HV_L~ 0.31 Å) of the free and ligand-bound Fab ADD056 suggests that the ligand binding is facilitated by the latter strategy, a hypothesis that contradicts the narrow nature of the entrance of the tunnel-like binding site. Finding a secondary portal that provides a solvent escape route explains this apparent paradox. Such resolution of the solvent-imposed binding constraints is rare. Only a few fatty acid binding proteins are prominent examples of systems with solvent escape paths.[27,28] In the case of Fab ADD056, the surface of the channel has amphiphilic properties that prevents exceedingly strong solvent binding and instead allows the molecules to pass through. Two residues, $Ser97_H$ and $Ser106_H$, may aid the process by tumbling between alternative side chain conformations and, thereby, shuttling water.

It is interesting to note that secondary entry portals have been observed in several proteins from different families that bind folate and its analogue methotrexate. For instance, in the structure of human folate receptor α we found a narrow channel that extents perpendicularly to the center of the binding cavity and emerges on the surface with a small opening, although it was not indicated by the authors.[29] Similarly to mAb ADD056, the receptor buries folate in a deep narrow cavity and establishes multiple hydrogen bonds with the ligand's pteroate moiety. The bond distribution is geometrically similar to the

dx.doi.org/10.1021/bi5001382 | Biochemistry 2014, 53, 3719−3726

hydrogen bond network involved with the DA-pteridine group in the methotrexate:Fab ADD056 complex.

In the dihydrofolate reductase from *E. coli*, we found a combination of two structural options: an open entrance area and a secondary portal. Even though the active site of the enzyme has a tunnel-like structure to accommodate its cofactor NADP, the folate pteroate group reaches into a cavity that features a solvent portal.[30] Among antibodies, a camelidae IgG against methotrexate binds the hapten in a site that looks like a partially closed groove, which allows easy solvent removal.[31] In contrast to mAb ADD056, this antibody forms hydrogen bonds over the whole length of the molecule, including the glutamic acid group.

Overall, directional displacement of the solvent seems to be a common mechanism for binding of folate and its analogues due to the biamphiphilic nature of these molecules. The pteroate/pteridin head moiety and the glutamic acid tail are much more hydrophilic than the middle section of the molecule around the pMA-benzoate. The complementary properties of the binding site increase the hydrophobic tendencies of this area and perhaps add an electrostatic barrier to the steric restraints that hinder solvent molecules from passing. Thus, a secondary water portal provides a solution to a strict geometric limitation imposed by a rigid binding site and can be considered as an indication of convergent evolution of folate-binding macromolecules.

CONCLUSION

The present study provides detailed insight into the binding of methotrexate to mAb ADD056 which is used to determine methotrexate levels in blood serum. The high affinity of this antibody can be explained by a few localized interactions between the protein matrix and the ligand's DA-pteridine moiety and its particular geometry. The binding site of mAb ADD056 is deep, narrow and extremely rigid, which prevents counterdirectional diffusion of solvent from the cavity. Therefore, the fast association rate of the complex formation can be explained by the presence of a water channel, which provides an escape route for solvent molecules displaced by the ligand. This finding suggests a new dimension in generating diversity in adaptive immunity. In fact, CDR H3 of mAb ADD056 plays an important structural role in formation of the channel. This hypervariable region is particularly prone to somatic mutations in the course of affinity maturation.[1,12,32] Therefore, the structural involvement of this hypervariable region in formation of the water channel suggests that the channel has evolved as a result of somatic mutations. It was recently shown that somatic mutations outside of the binding site play an important role in keeping thermodynamic stability of the immunoglobulin variable domains during affinity maturation *in vivo*.[33] Providing solvent escape routes is another example of how remote mutations can have an effect on antigen binding. Our observation adds a new component to affinity and on-rate maturation strategies of antibodies in vitro and may guide antibody engineering efforts in a new direction by rationally designing solvent escape routes through secondary portals.

Protein data bank accession code coordinates and structure factors of the anti-methotrexate Fab ADD056 in its apo- and bound forms have been deposited in the RCSB Protein Data bank with access codes 4OCX and 4OCY.

AUTHOR INFORMATION

Corresponding Author

*E-mail: sergey.tetin@abbott.com. Tel.: 847-935-4661. Fax: 847-935-6498. Address: D-09MC, AP-20, Abbott Laboratories, 100 Abbott Park Road, Abbott Park, Illinois 60064-6016, United States.

Present Address

[§]Structural Biology, Discovery Chemistry and Technology, AbbVie, North Chicago, Illinois 60064, United States.

Author Contributions

[⊥]These authors contributed equally to this work.

Notes

The authors declare no competing financial interest.

ACKNOWLEDGMENTS

X-ray diffraction data were collected at beamline 17-BM in the facilities of the Industrial Macromolecular Crystallography Association Collaborative Access Team (IMCA-CAT) at the Advanced Photon Source. These facilities are supported by the companies of the Industrial Macromolecular Crystallography Association.

REFERENCES

(1) Padlan, E. A. (1994) Anatomy of the antibody molecule. *Mol. Immunol. 31*, 169−217.

(2) Edmundson, A. B., Guddat, L. W., Shan, L., Fan, Z. C., and Hanson, B. L. (1994) Structural aspects of conformational changes in ligand binding by antibody fragments. *Res. Immunol. 145*, 56−61.

(3) Landsteiner, K. (1945) *The Specificity of Serological Reactions*, Harvard University Press, Cambridge, MA.

(4) Herron, J. N., He, X. M., Ballard, D. W., Blier, P. R., Pace, P. E., Bothwell, A. L., Voss, E. W., Jr., and Edmundson, A. B. (1991) An autoantibody to single-stranded DNA: comparison of the three-dimensional structures of the unliganded Fab and a deoxynucleotide-Fab complex. *Proteins 11*, 159−175.

(5) Guddat, L. W., Shan, L., Anchin, J. M., Linthicum, D. S., and Edmundson, A. B. (1994) Local and transmitted conformational changes on complexation of an anti-sweetener Fab. *J. Mol. Biol. 236*, 247−274.

(6) Rini, J. M., Schulze-Gahmen, U., and Wilson, I. A. (1992) Structural evidence for induced fit as a mechanism for antibody-antigen recognition. *Science 255*, 959−965.

(7) Stanfield, R. L., Takimoto-Kamimura, M., Rini, J. M., Profy, A. T., and Wilson, I. A. (1993) Major antigen-induced domain rearrangements in an antibody. *Structure 1*, 83−93.

(8) Jeffrey, P. D., Strong, R. K., Sieker, L. C., Chang, C. Y., Campbell, R. L., Petsko, G. A., Haber, E., Margolies, M. N., and Sheriff, S. (1993) 26−10 Fab-digoxin complex: affinity and specificity due to surface complementarity. *Proc. Natl. Acad. Sci. U. S. A. 90*, 10310−10314.

(9) Chan, E. S., and Cronstein, B. N. (2010) Methotrexate–how does it really work? *Nat. Rev. Rheumatol. 6*, 175−178.

(10) Tian, H., and Cronstein, B. N. (2007) Understanding the mechanisms of action of methotrexate: implications for the treatment of rheumatoid arthritis. *Bull. NYU Hosp. Jt. Dis. 65*, 168−173.

(11) Visentin, M., Zhao, R., and Goldman, I. D. (2012) The antifolates. *Hematol./Oncol. Clin. North Am. 26*, 629−648 ix..

(12) Schroeder, H. W., Jr., Zemlin, M., Khass, M., Nguyen, H. H., and Schelonka, R. L. (2010) Genetic control of DH reading frame and its effect on B-cell development and antigen-specifc antibody production. *Crit. Rev. Immunol. 30*, 327−344.

(13) Vonrhein, C., Flensburg, C., Keller, P., Sharff, A., Smart, O., Paciorek, W., Womack, T., and Bricogne, G. (2011) Data processing and analysis with the autoPROC toolbox. *Acta Crystallogr., Sect. D: Biol. Crystallogr. 67*, 293−302.

(14) Vagin, A., and Teplyakov, A. (1997) MOLREP: an automated program for molecular replacement. *J. Appl. Crystallogr. 30*, 1022−1025.
(15) Winn, M. D., Ballard, C. C., Cowtan, K. D., Dodson, E. J., Emsley, P., Evans, P. R., Keegan, R. M., Krissinel, E. B., Leslie, A. G. W., McCoy, A., McNicholas, S. J., Murshudov, G. N., Pannu, N. S., Potterton, E. A., Powell, H. R., Read, R. J., Vagin, A., and Wilson, K. S. (2011) Overview of the CCP4 suite and current developments. *Acta Crystallogr., Sect. D: Biol. Crystallogr. 67*, 235−242.
(16) Emsley, P., Lohkamp, B., Scott, W. G., and Cowtan, K. (2010) Features and development of Coot. *Acta Crystallogr., Sect. D: Biol. Crystallogr. 66*, 486−501.
(17) Wlodek, S., Skillman, A. G., and Nicholls, A. (2006) Automated ligand placement and refinement with a combined force field and shape potential. *Acta Crystallogr., Sect. D: Biol. Crystallogr. 62*, 741−749.
(18) Murshudov, G. N., Skubak, P., Lebedev, A. A., Pannu, N. S., Steiner, R. A., Nicholls, R. A., Winn, M. D., Long, F., and Vagin, A. A. (2011) REFMAC5 for the refinement of macromolecular crystal structures. *Acta Crystallogr., Sect. D: Biol. Crystallogr. 67*, 355−367.
(19) Bricogne G, B. E., Brandl, M., Flensburg, C., Keller, P., Paciorek, W., Roversi, P., Sharff, A., Smart, O. S., Vonrhein, C., Womack, T. O. (2011) *BUSTER*, Version 2.10.0, Global Phasing Ltd., Cambridge, UK.
(20) Grote, J., Beligere, G., and Rege, S. (2012) Methodology for the regiospecific synthesis and characterization of methotrexate conjugates. *Tetrahedron Lett. 53*, 5331−5334.
(21) Tetin, S. Y., and Hazlett, T. L. (2000) Optical spectroscopy in studies of antibody-hapten interactions. *Methods 20*, 341−361.
(22) Chothia, C., and Lesk, A. M. (1987) Canonical structures for the hypervariable regions of immunoglobulins. *J. Mol. Biol. 196*, 901−917.
(23) Al-Lazikani, B., Lesk, A. M., and Chothia, C. (1997) Standard conformations for the canonical structures of immunoglobulins. *J. Mol. Biol. 273*, 927−948.
(24) North, B., Lehmann, A., and Dunbrack, R. L., Jr. (2011) A new clustering of antibody CDR loop conformations. *J. Mol. Biol. 406*, 228−256.
(25) Weber, G. (1965) The binding of small molecules to proteins. In *Molecular Biophysics: Proceedings of an international summer school held in Squaw Valley, California* (Weissbluth, B. P. a. M., Ed.), pp 369−396.
(26) Pecht, I. (1982) Dynamic Aspects of Antibody Function. In *The Antigens* (Sela, M., Ed.), pp 1−63, Academic Press, Salt Lake City, UT.
(27) Zanotti, G., Scapin, G., Spadon, P., Veerkamp, J. H., and Sacchettini, J. C. (1992) Three-dimensional structure of recombinant human muscle fatty acid-binding protein. *J. Biol. Chem. 267*, 18541−18550.
(28) Young, A. C., Scapin, G., Kromminga, A., Patel, S. B., Veerkamp, J. H., and Sacchettini, J. C. (1994) Structural studies on human muscle fatty acid binding protein at 1.4 A resolution: binding interactions with three C18 fatty acids. *Structure 2*, 523−534.
(29) Chen, C., Ke, J., Zhou, X. E., Yi, W., Brunzelle, J. S., Li, J., Yong, E. L., Xu, H. E., and Melcher, K. (2013) Structural basis for molecular recognition of folic acid by folate receptors. *Nature 500*, 486−489.
(30) Bystroff, C., Oatley, S. J., and Kraut, J. (1990) Crystal structures of Escherichia coli dihydrofolate reductase: the NADP+ holoenzyme and the folate.NADP+ ternary complex. Substrate binding and a model for the transition state. *Biochemistry 29*, 3263−3277.
(31) Fanning, S. W., and Horn, J. R. (2011) An anti-hapten camelid antibody reveals a cryptic binding site with significant energetic contributions from a nonhypervariable loop. *Protein Sci. 20*, 1196−1207.
(32) Kim, S., Davis, M., Sinn, E., Patten, P., and Hood, L. (1981) Antibody diversity: somatic hypermutation of rearranged VH genes. *Cell 27*, 573−581.
(33) Wang, F., Sen, S., Zhang, Y., Ahmad, I., Zhu, X., Wilson, I. A., Smider, V. V., Magliery, T. J., and Schultz, P. G. (2013) Somatic hypermutation maintains antibody thermodynamic stability during affinity maturation. *Proc. Natl. Acad. Sci. U. S. A. 110*, 4261−4266.